Web buckling behavior of FRP composite box-beams: Governing parameters and their effect

M. Kasiviswanathan* and Akhil Upadhyay[a]

Department of Civil Engineering, Indian Institute of Technology Roorkee, Roorkee 247667, India

Abstract. The lightweight superstructure is beneficial for bridges in remote areas and emergency erection. In such weight-sensitive applications, the combination of fiber-reinforced polymer (FRP) as a material and box-beams as a structural system have enormous scope. This combination offers various advantages, but as a thin-walled structure, their designs are often governed by buckling criteria. FRP box-beams lose their stability either by flange or web buckling mode. In this paper, the web buckling behavior of simply supported FRP box-beam subjected to transverse load has been studied by modeling full box-beam to consider the effect of real state of stress (stress variation in length direction) and boundary conditions (rotational restraint at web-flange junction). A parametric study by varying the sectional geometry and fiber orientation is carried out by using ANSYS software. The accuracy of the FE models was ensured by verifying them against the available results provided in the literature. With the help of developed database the influential parameters (i.e., α_s, β_w, δ_w and γ) affecting the web bucklings are identified. Design trends have been developed which will be helpful to the designers in the preliminary stage. Finally, the importance of governing parameters and design trends are demonstrated through pedestrian bridge design.

Keywords: FRP box-beam; web buckling; rotational restraint; stability problem; FE analysis

1. Introduction

In recent times, the application of structures made of laminated composites is increased in various engineering fields such as civil, marine, and aerospace. Composites offer many advantages over traditional materials (concrete and steel), for example, high strength and stiffness, corrosion resistance, lightweight, and tailoring of the material to a specific application (Ranganathan and Mantena (2003)). Meanwhile, box-beam finds many uses in civil engineering because of their bending resistance, sectional integrity and high torsional rigidity. The demand for high strength and stiffness for lightweight bridges lead the researchers to explore the combination of FRP and box-girder (Upadhyay and Kalyanaraman (2003)). FRP box-beams are made by thin panels, because of thin-walled sectional property and relatively low stiffness to strength ratio of FRP, beams lose their stability before reaching their material strength limit states (Rasheed *et al*. (2017), Zhan and Wu (2018) and Zhan *et al*. (2018)). Accurate prediction of buckling strength is essential

---

*Corresponding author, Ph.D., E-mail: km@ce.iitr.ac.in
[a]Professor, E-mail: akhilfce@iitr.ac.in

for the reliable, efficient, and safe design of thin-walled FRP box-beams. Hence, special attention needs to be given to the design of FRP box-beams.

Generally, in FRP box-beams, two types of buckling are possible, i.e., flange and web buckling. To estimate the flange and web buckling strength of FRP beams, most of the earlier researchers have used a discrete plate approach. In which, instead of modeling full box-beam, individual panels are modeled with idealized and approximate boundary restraints and are subjected to uniform in-plane forces. This method was introduced by Bleich (1952) for an isotropic panel. Then, this methodology has been followed by many researchers. Sathiyaseelan and Baskar (2012) carried out a numerical study for steel plate subjected to combined shear and tensile stresses and developed interaction curves for a simply supported plate. Taleb *et al*. (2015) have carried out buckling studies to ensure simply supported boundary conditions at a web-flange junction. Serror *et al*. (2016) have studied the web plate subjected to in-plane linearly varying compression with different loading patterns, they performed a numerical study and found the influential parameter, but they assumed simply supported boundary condition at the web-flange junction, in reality, it is different and discussed below in this section. Later, researchers have expanded this methodology for orthotropic material. Plates subjected to uni-axial compression load, shear load, in-plane linearly varying load and their combination are studied by Lekhnitskii (1968), Barbero (1993), Whitney (1987), Bank and Yin (1996), Qiao *et al*. (2001), Kollar (2002, 2003), Qiao and Zou (2002, 2003), Qiao and Shan (2005), Tarjan *et al*. (2010a), Qiao and Huo (2011). Orthotropic panels with simple boundary un-loaded edges (free, simply-supported, and clamped) are studied by Lekhnitskii (1968), Whitney (1987), and Barbero and Raftoyiannis (1993). However, realistic boundary condition lies between two extreme boundary conditions such as simply-supported and clamped. Thus, to consider this realistic boundary condition, Bank and Yin (1996) and Qiao *et al*. (2001) have attempted to solve the problems of an orthotropic panel with rotationally restrained un-loaded edges, but they didn't achieve the explicit expressions. The first set of closed-form equations with the incorporation of rotational restraint was presented by Kollar (2002, 2003). He also proposed the simplified approach to assess the buckling capacity of different FRP profiles based on the existing equations which were proposed by other researchers for orthotropic plates. For axially loaded box-beam, Kollar (2003) compared his results with available literature results (numerical and experimental), but the web buckling of box-beam under transverse load is not covered in this work.

Web buckling occurs in presence of bending compression and in-plane shear load. Explicit closed-form equations for panels subjected to bending stresses and shear stresses are needed to calculate the web buckling strength of laterally loaded FRP box-beams. Qiao and Zou (2003) have studied plate subjected to bending stresses with consideration of rotational restraint. However, Tarjan *et al*. (2010a) have reported that these equations predict infinite buckling load for a few cases, which is unrealistic. Tarjan *et al*. (2010a) have developed the closed-form expression for discrete plates subjected to bending, and shear stresses with consideration of rotational restraint along the un-loaded edges. Additionally, they tabulated the available equations for the orthotropic plate. Based on these closed-form equations, Tarjan *et al*. (2010b) have studied the web buckling of FRP box-beam under transverse loads. They compared their results with FEA results. For bending, a better match is observed with FEA results, but for shear and combined load, the considerable difference is found. Notably, for the shear load case, the % difference has increased up to 25%. One of the main reported reasons was the presence of moment gradient which brings variation in shear stress and the same cannot be handled using available closed-form solutions. Liu *et al*. (2014) have also studied the web buckling of FRP box-beam under transverse loads, but their
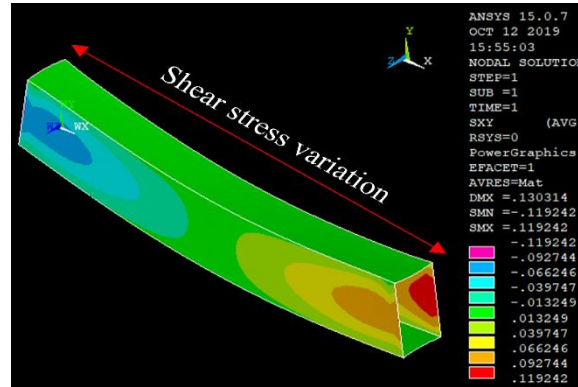
Fig. 1 Shear stress variation in box-beam

expressions are in implicit form. Equations proposed by Kollar (2003), Tarjan *et al*. (2010a) and Liu *et al*. (2014) are simple, but it increases the calculation effort as a result of required independent calculation for flange and web elements. To reduce this calculation effort, Cardoso *et al*. (2014) have used a full section buckling approach but they studied only concentrically compression loaded FRP sections (e.g., angles, I-shaped, channels and rectangular tubes).

From the literature, it is cleared that limited studies have been reported on the local buckling of laminated FRP box-beams as based on full section buckling approach. To calculate the web buckling strength of FRP beams, most of the previous researchers have used discrete plate approach. In reality, these web plates are part of the box-beam, and their stresses vary in length direction which brings significant changes in buckling behavior. Fig. 1 shows the shear stress variation in transversely loaded simply supported box-beam. Further, consideration of elastic restraint at web-flange junction leads to more accurate results. Hence, in this paper real state of stress and boundary condiditons are taken into account by modeling and analyzing full box-beam with the help of finite element software 'ANSYS 15'. Studies are carried out by changing the fiber orientation and geometry of various elements of box-beam. Parameters influencing the web buckling are identified and their significance have been discussed with the help of generic curves.

2. Need for studies and basic plan

As discussed in the last section, most of the previous researchers have used discrete plate technique to study the web buckling behavior of FRP box-beam. In which, plates are subjected to bending compression or in-plane shear load and their un-loaded edges are restraint either by using simply support or clamped support. In reality, stresses are varying in the longitudinal direction and buckling panels receive considerable rotational restraint from supporting panels. In the present work, a comparative study is carried out to check the performance of a discrete plate based closed-form equation in the prediction of the web buckling coefficient of FRP box-beams. A few FRP box-beams, having various extreme possible combination of fiber orientation in web and flange, are modeled in present work using FEM to get web buckling coefficients, and the same are compared by using discrete plate equations reported by Tarjan *et al*. (2010b). Table 1 shows the result comparison. The last column of Table 1, clearly indicates a considerable error in discrete

Table 1 Comparison of buckling coefficient by FEA and Tarjan *et al*. (2010b)

L=2000 (mm), b_f=147 (mm), b_w=225 (mm), t_f=5 (mm), t_w=3 (mm)				
		Web buckling coefficient (K)		% Error
θ_f	θ_w	FEA (present work) (a)	Tarjan *et al*. (2010b) (b)	$\left(\dfrac{b\text{-}a}{a}\right)*100$
0°	0°	1.34	1.78	32.94
	±45°	1.543	2.05	33.02
	90°	1.94	1.80	-6.97
±45°	0°	1.32	1.94	47.24
	±45°	1.55	2.26	45.94
	90°	2.07	1.95	-5.75
90°	0°	1.30	1.99	53.54
	±45°	1.54	2.19	39.58
	90°	1.97	1.94	-1.07

plate based predictions. In some cases, the error is on the unconservative side. This observation suggests the limitations of these solutions to tackle real boundary conditions and especially the state of stress existing in FRP box-beams, and it brings out the need for further studies in this regard. Further, due to the involvement of large number of variables understanding the web buckling behavior of laminated FRP composite box-beam is quite tedious. Hence, to develop a better understanding of web buckling with consideration of the real state of stress and boundary conditions, governing paramters are need to be identified. Therefore, in this study, the finite element based numerical study has been conducted by changing the geometry and fiber orientation of flange and webs. Based on the studies, some parameters affecting the web buckling behavior are discussed.

3. Numerical study

3.1 General

Numerical models were developed by using FEA software ANSYS (2003). To ensure the accuracy of the finite element models, results available in the literature were verified. An extensive parametric study is conducted to generate the database to identify a governing parameters to understand the web buckling behavior of FRP box-beams.

3.2 Element type and mesh convergence study

The widely adopted element shell is used to model the FRP composite panels. Shell element is well suited for layered applications (modeling composite shells or sandwich construction). The first order shear deformation theory is implemented in the element (shell281) chosen to create a discrete beam model. Element shell281 has been successfully used by other researchers in numerical modeling of FRP beams and columns (Chandak *et al*. (2010), Debski *et al*. (2013) and
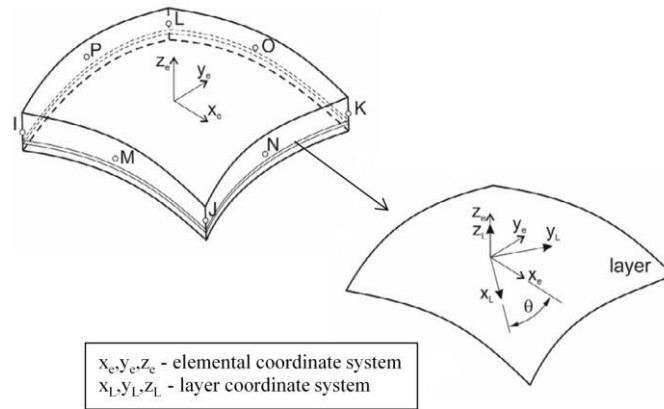
Fig. 2 Employed multi-layered eight-node shell element - shell281 (ANSYS (2003))

Kubiak *et al.* (2016)). This element has 8 nodes and 6 degrees of freedom at each node: translation in the X, Y and Z direction and rotation about X, Y and Z axes. The beam flange and web component thickness is defined as element attributes, which also allows one to define a number of layers, their thicknesses, material properties and orientations of principal axes of orthotropy (θ angle see Fig. 2) for each layer.

In finite element modeling, smaller size elements provide accurate results but it increases the computational time. Hence, to manage the computing source as well as accuracy, mesh convergence study was performed by performing linear elastic eigenvalue buckling analysis. Based on the results of the mesh convergence study, element size<50 mm has been chosen for box-beams. The number of elements used in the current study ranges from 3200-10956.

3.3 Loading and boundary conditions

Simply supported FRP box-beams subjected to transverse load is used for the parametric study to obtain web buckling strength. Loads are applied at the web-flange junctions as depicted in Fig. 3. To create the simply support condition, Y and Z axis translation of all nodes are constrained at both ends. At one end, nodes at the center of the web are restrained for translation along the X-axis or length direction to avoid the rigid body movement. The adopted boundary condition about X, Y and Z plane is shown in Fig. 3.

3.4 Elastic analysis

The numerical model was developed by using centerline dimensions of the cross-sections. To predict the web buckling strength of box-beams eigenvalue buckling analysis was performed. In this study, web buckling mode is kept as a dominant buckling mode. The typical web buckling mode obtained from the elastic analysis is shown in Fig. 4.

3.5 Verification

FE modeling needs more care while defining material properties, fiber orientations, mesh sizes,
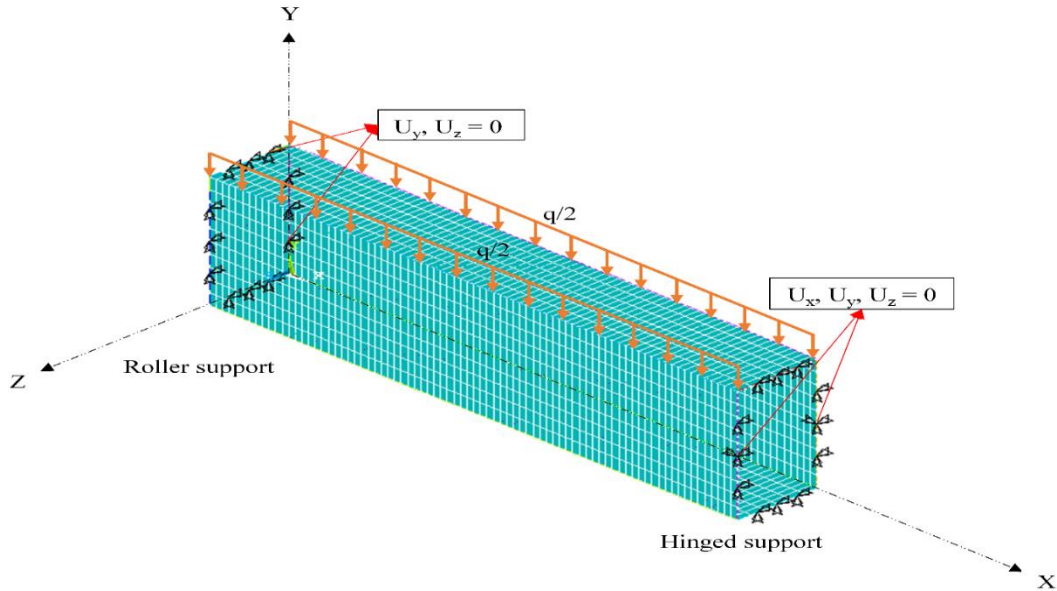
Fig. 3 Finite element boundary conditions and load application of box-beam

(a)

(b)   (c)
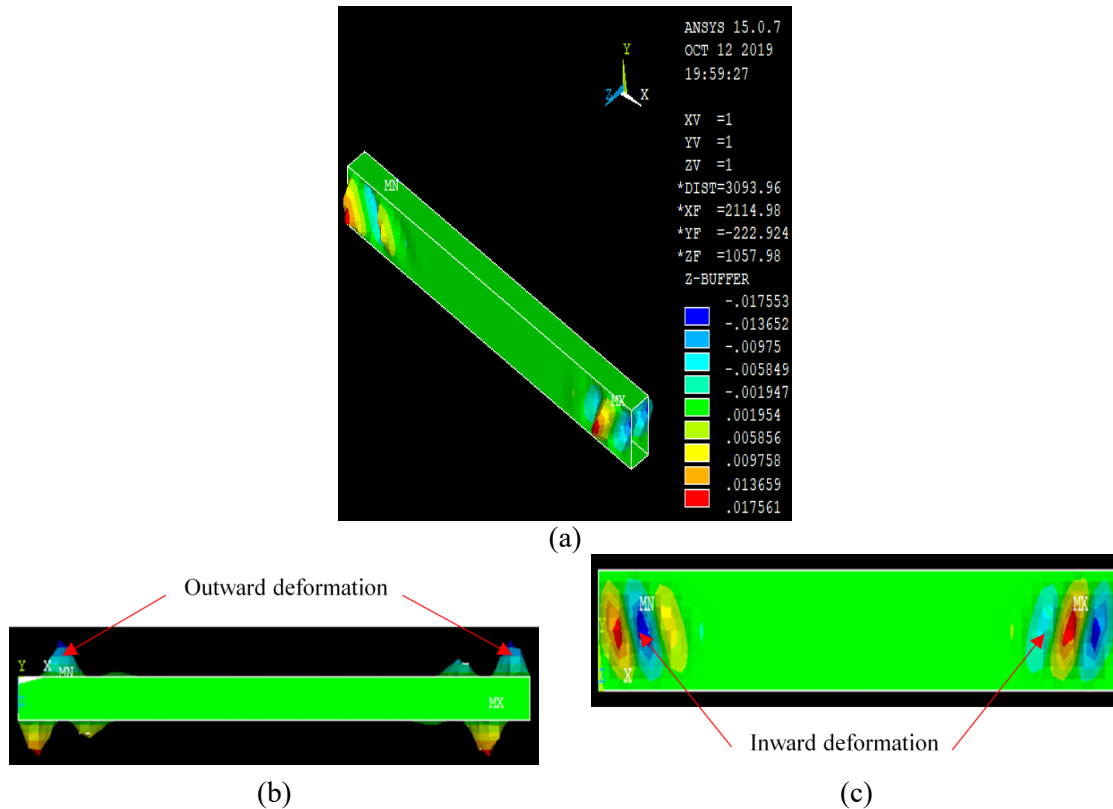
Fig. 4 Buckling pattern corresponding to first Eigenvalue (beam size-300 × 600 × 5000) (a) Isometric view (b) Top view (c) Side view

Table 2 Verification of FE model

Dimensions in mm	Load case	N_{cr} (kN/m)		% Difference ((b-a)/b)*100
		FE analysis		
$b_w \times t_w \times b_f \times t_f$		Liu *et al.* (2014) (a)	Present study (b)	
$200 \times 4 \times 150 \times 8$	Uniform compression	523.670	511.158	-2.40
$225 \times 3 \times 147 \times 5$	Four-point bending	11.603	11.627	0.20
$225 \times 3 \times 147 \times 5$	Five-point bending	7.736	7.770	0.43

Table 3 Cross-sectional dimensions and fiber orientations of parametric study

θ_f	θ_w	b_w (mm)	t_w (mm)	Number of simulations	
L=5000 (mm), b_f=300 (mm), t_f=15 (mm)					
				SL	TL
$(0°/0°)_s$	$(0°/0°)_s$	{500, 600, 700}	{1, 1.5, 2, 3, 4}	15	15
	$(\pm45°)_s$	{500, 600, 700}	{1, 1.5, 2, 3, 4}	15	15
	$(90°/90°)_s$	{500, 600, 700}	{1, 1.5, 2, 3, 4}	15	15
$(\pm45°)_s$	$(0°/0°)_s$	{500, 600, 700}	{1, 1.5, 2, 3, 4}	15	15
	$(\pm45°)_s$	{500, 600, 700}	{1, 1.5, 2, 3, 4}	15	15
	$(90°/90°)_s$	{500, 600, 700}	{1, 1.5, 2, 3, 4}	15	15
$(90°/90°)_s$	$(0°/0°)_s$	{500, 600, 700}	{1, 1.5, 2, 3, 4}	15	15
	$(\pm45°)_s$	{500, 600, 700}	{1, 1.5, 2, 3, 4}	15	15
	$(90°/90°)_s$	{500, 600, 700}	{1, 1.5, 2, 3, 4}	15	15
			Total	135+135=270	

SL – symmetric load, *TL* – torsional load

and constraints. Establishing the accuracy of the finite element model is essential before it is used for the analysis. Hence, to ensure the accuracy of the current models of the box-beams, web buckling strength of box-beam reported by Liu *et al*. (2014) are verified. To verify the Liu *et al*. (2014) results, material properties D_{11}=751.12 Nm, D_{22}=355.33 Nm, D_{12}=141.38 Nm and D_{66}=112.34 Nm are used for both flange and webs. Table 2 shows the verified beam geometry and load details. From the comparison of results shown in the table, it can be observed that the buckling load obtained from the present study closely matches with Liu *et al*. (2014) results. It implies that defined material properties, constraints and load application for simulated Liu *et al*. (2014) beam models are correct. Hence, in the present work, a parametric study is performed with desired sectional geometry, material properties and loading conditions.

4. Parametric study

In the parametric study, laminated composite box-beams subjected to transverse load was used. In all the analyses, web buckling is kept as the dominant buckling mode. It is achieved by keeping the slenderness value of flange $((b/t)_f)$ lower than web slenderness value $(b/t)_w$. In this study, minimum b/t values considered for flange and web are 20 and 125, respectively, beams having
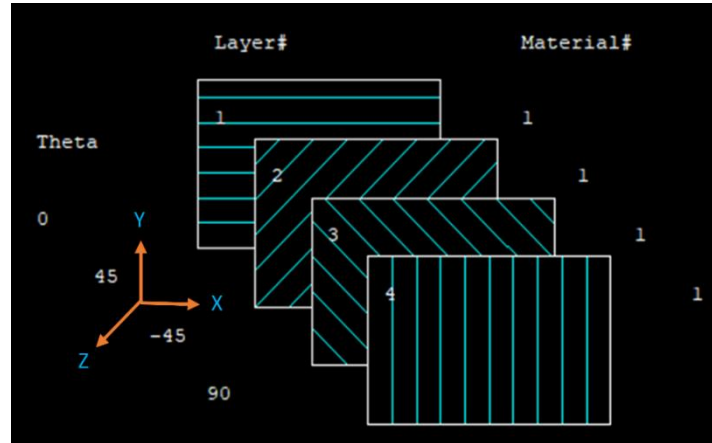
Fig. 5 Orientations of fibers (0°, ±45°, 90°) simulated in ANSYS

Table 4 Lamina material properties (Stroud and Agranoff (1976))

E_1 (GPa)	E_2 (GPa)	G_{12} (GPa)	ρ (kg/m^3)	v_{12}	v_{21}
145	16.5	4.48	1520	0.314	0.037

web slenderness values $((b/t)_w)$ ranging from 125 to 700 are used to bring out the effect of rotational restraint provided by a flange on web buckling. Five different flange thicknesses and three different flange widths are used to arrive at this wide range of slenderness ratios. Three types of laminates are considered for both web and flange, i.e., $[(0°/0°)_2]_s$, $[(\pm45°)_2]_s$ and $[(90°/90°)_2]_s$ to bring out the extreme values of orthotropy ratio. The orientations of fibers as simulated in ANSYS is shown in Fig. 5. For all simulations, the length of the beam and width and thickness of the flanges are kept constant. The considered fiber orientations and geometry of the beam are shown in Table 3. The geometric details of the beam cross-sections are shown in Fig. 3.

Graphite-epoxy material is used to model the box-beam components (flange and web). Material properties used in this study are taken from the Stroud and Agranoff (1976). Table 4 shows the mechanical properties of graphite-epoxy. The web buckling strengths of the FRP box-beams obtained from the numerical study were used to arrive the governing parameters and design trends.

5. Parameters influencing web buckling

Under transverse load, because of high strength/stiffness ratio, FRP box-beams lose their stability either by the flange or web buckling. Web buckling has become a dominant buckling mode when flange has enough resistance against compression. Many researchers have studied web buckling, but most of them have used the discrete plate approach. In reality, webs are the part of box-beams and their buckling strength significantly influenced by the state of stress and boundary condition at the web-flange junction. Hence, to understand the influence of this real state of stress and boundary conditions on web buckling, influential parameters need to be identified. In literature, for the standard state of stress and boundary condition, governing parameters are available in the closed-form solutions, but we cannot use as it is because in current problem state

of stress and boundary conditions are not the same. Because of the above fact, in this study, based on the generated database (based on the full box-beam analysis) and existing knowledge in this area, parameters influencing the web bucklings are identified. The details of parameters and their genesis are as follows. Firstly, Housner and Stein (1975) have studied the shear loaded panel and proposed local buckling equation that is

$$N_{xy} = k_s \frac{\pi^2 \sqrt[4]{D_{11}D_{22}^3}}{b^2} \tag{1}$$

Stroud and Agranoff (1976) have also presented a similar type of equation for local buckling for shear loaded panel based on the shear buckling parameter. From the studies mentioned above, it can be observed that D_{22} plays a significant role in web buckling as compared to the other bending stiffnesses. Hence, herein, extensive numerical studies have been carried out to quantify the significance of D_{22} against shear buckling. As a consequence, in the present study, α_s is taken as a flexural parameter and it's defined as follows.

$$\alpha_s = \frac{(D_{11}D_{22}^3)_w^{\frac{1}{4}}}{(b_w)^2} \tag{2}$$

The buckling behavior of the plate depends on received rotational restraint from supporting plates. Rotational restraint depends on the geometrical and transverse flexural properties of both supporting and supported plates. The effect of rotational restraint on flange buckling was extensively studied by Kasiviswanathan and Upadhyay (2018) and they observed maximum increases in buckling stress due to rotational restraint is around 60%. In the present work, to study the influence of rotational restraint on web buckling, the rotational restraint parameter (β_w) is defined as follows.

$$\beta_w = \frac{D_{22f}b_w}{D_{22w}b_f} \tag{3}$$

The parameter β_w helps to understand the effect of flange provided rotational restraints on web buckling. When β_w is small, restraint from flange to web is low; as a result, the web behaves like a simply supported plate. In contrast, when β_w is higher, webs behaves like a clamped plate because restraints from flange to web is high.

The parameter δ_w is the ratio of extensional stiffness to the shear stiffness of flange to the web. Mallela and Upadhyay (2009) have defined the parameter (A_{11}/A_{66}) and shown its effect on the shear loaded panel. In this work, it is modified to incorporate the influence of extensional to shear stiffness of flange and web on the web buckling of FRP box-beam. The modified parameter δ_w is defined below.

$$\delta_w = \frac{(A_{11}/A_{66})_f}{(A_{11}^2/(A_{22}A_{66}))_w} \tag{4}$$

Further, torsional rigidities of the panel also influence the buckling behavior of webs under un-symmetrical load cases, the parameter γ is defined in present study to take care of torsional rigidities of the webs.

(a)

(b)

(c)
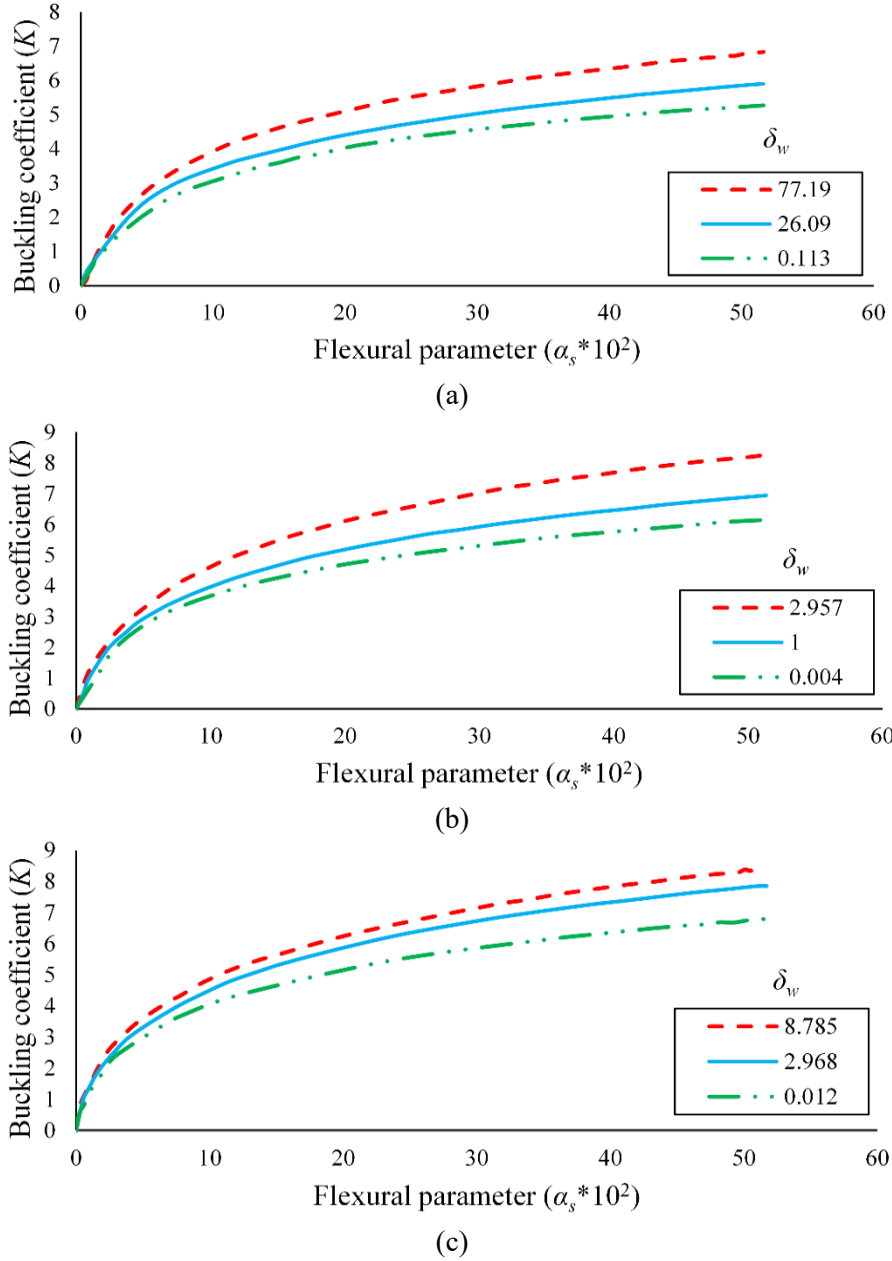
Fig. 6 Variation of buckling coefficient (K) with α_s for different δ_w values (a) $(D_{11}/D_{22})_f = 8.790$ (b) $(D_{11}/D_{22})_f = 1$ (c) $(D_{11}/D_{22})_f = 0.114$

$$\gamma = \left(\frac{D_{22}}{D_{11}} \right)_w^{\frac{1}{4}} \left(D_{12} + 2D_{66} \right)_w \tag{5}$$
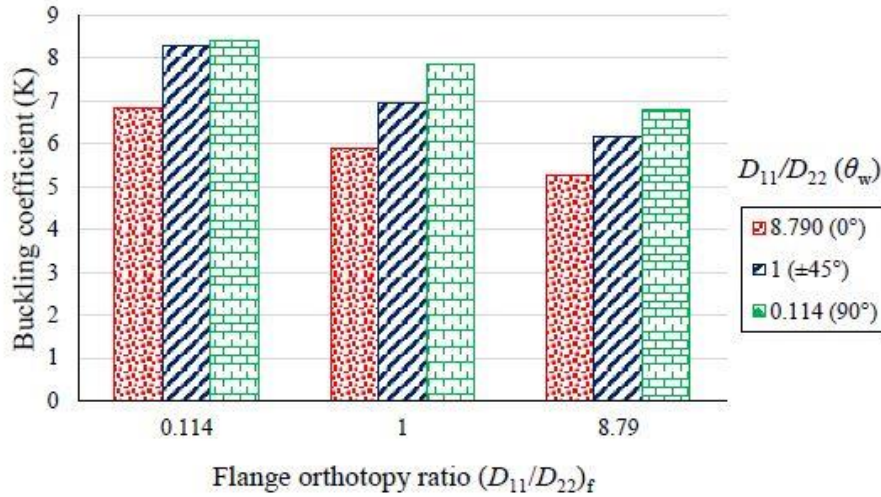
Fig. 7 Effect of transverse rigidity on buckling coefficient (K)
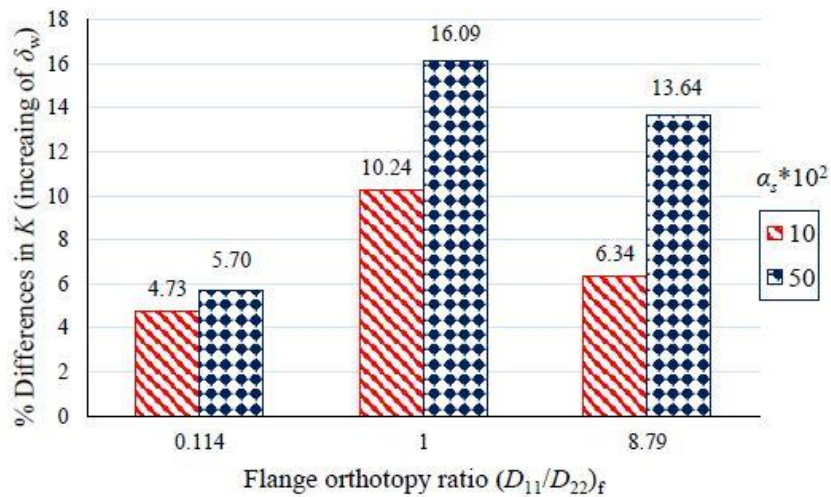
Fig. 8 Influence of δw significance on buckling coefficient (K) for different αs values

Where, in the above equations (1 to 5), b is the width of the elements and subscripts f and w refer to the flange and web of box-beams. A-terms refer to the shear and extensional stiffness, and D-terms refers to the bending stiffness of the classical laminated plate theory.

5.1 Effect of the flexural parameter (α$_s$) and shear stiffness parameter (δ$_w$)

As mentioned in the earlier section, the buckling resistance of shear loaded panel mainly depends on transverse rigidities (D_{22}) of laminate. Since the D_{22} role is high in buckling resistance, the influence of other bending stiffness in the laminate (symmetrically balanced) such as D_{11}, D_{12}

and D_{16} are relatively small. This section shows the influence of bending stiffnesses on web buckling with the aid of flexural parameter (α_s).

Fig. 6 shows the variation of the buckling coefficient (K) with flexural parameter (α_s) for different shear stiffness parameter (δ_w). Figs. 6(a) - 6(c) corresponds to a different flange orthotropy ratio. In all the cases, flange buckling is excluded by providing thicker plate and beam depth is kept constant that is 500 mm. From these figures, it can be noticed that in the beginning, the buckling coefficient increases significantly with an increase in α_s. However, beyond a particular value of α_s, around 0.1, the rate of increase in buckling coefficient (K) decreases considerably with an increase in the flexural parameter. At a later stage, it can be observed that parameter δ_w plays an important role in increasing the buckling capacity; that is when flexural stiffness is high, panel requires adequate shear stiffness to produce the maximum buckling coefficient. Similar behavior is observed for beam depth 600 and 700 mm. Further, the transverse flexural rigidity (D_{22}) is more significant for shear buckling point of view. Web fiber orientation $90°$ and $±45°$ are giving a higher buckling coefficient, and the same can be observed from Fig. 7.

As aforesaid, δ_w is having more influence on buckling coefficient (K) at higher α_s. Fig. 8 shows the quantitative information about the influence of δ_w on K. The % increase in buckling coefficient (K) due to increasing of δ_w (when web fiber orientation is changed from $±45°$ to $90°$) is plotted against different $(D_{11}/D_{22})_f$ for two flexural parameter (α_s) values i.e. 0.1 and 0.5. From this Figure, it can be observed that the significance of δ_w is low at lower α_s value while it increases considerably at higher α_s value. The maximum increase in buckling coefficient due to δ_w in the present study is found to be around 16%.

5.2 Effect of rotational restraint parameter (β_w)

The buckling behavior of the web is sensitive to the boundary condition. For standard boundary conditions (clamped and simply supported), solutions are available in the literature. But, in reality, webs are the part of box-beam, and it is difficult to identify the received rotational restraint from the flange. In this work, the rotational restraint parameter (β_w) is defined to study the influence of rotational restraint on web buckling.

5.3 Effect of the torsional parameter (γ)

Under torsional loading, the beam cross-section will experience rotation as well as distortion. As a result, one web panel will deform in an upward direction while another one deforms in a downward direction. Distortion will introduce warping, and due to its restraint, longitudinal stresses will develop. The cross-section and deformed shapes of the beam are shown in Fig. 11. In the present study, torsional parameter γ is defined to explain the torsional buckling behavior of the beam.

Fig. 12 shows the variation of buckling coefficient (K) with torsional parameter (γ) for two load cases, i.e., symmetrical (*SL*) and torsional load (*TL*). Figs 12(a-f) corresponds to different beam depth (b_w). From these figures, it can be observed that in all torsional load cases buckling coefficient is lower than the symmetrical load case coefficient, especially for a higher value of γ. This is due to additional shear resulting from torsion. In the presence of torsion loading, the performance of $±45°$ fibers in the web is better due to the higher value of torsional rigidities ($D_{12}+D_{66}$). For the same value of γ, $0°$ and $90°$ panels give a higher buckling coefficient (K) in comparison to $±45°$ due to the lower value of b/t ratio of these plates. However, for given b/t ratio γ
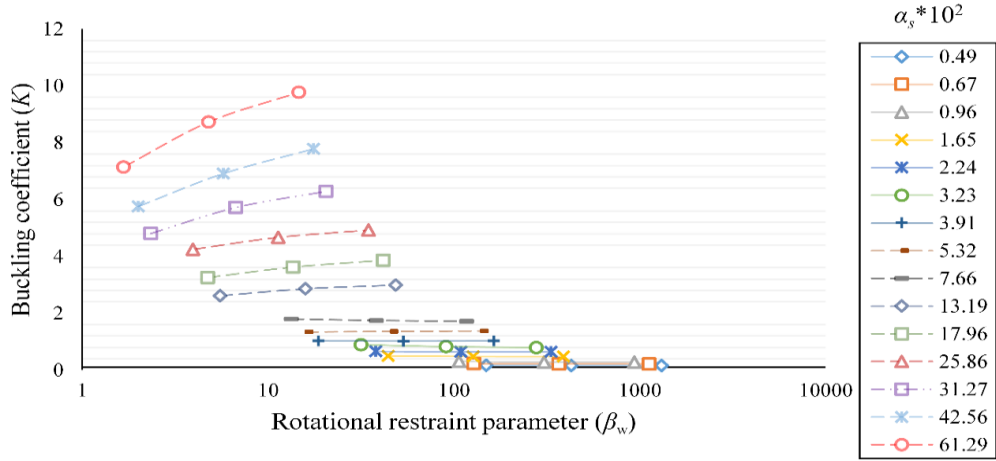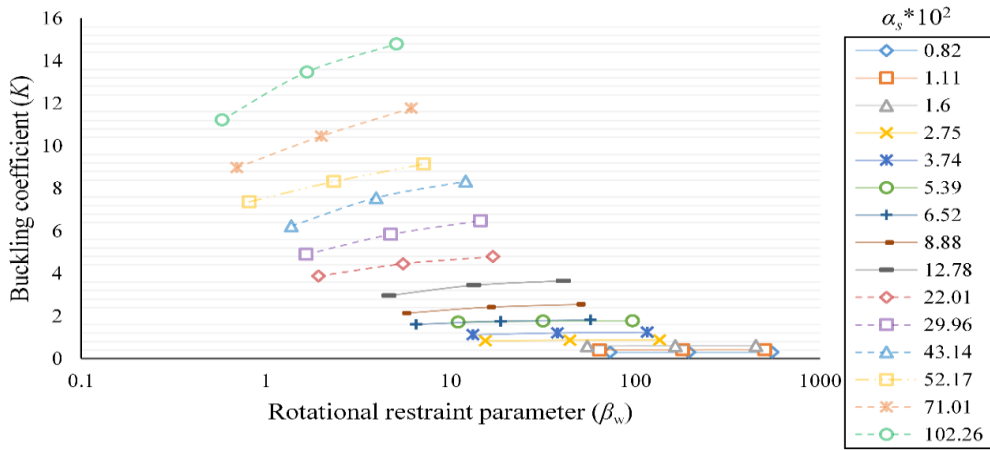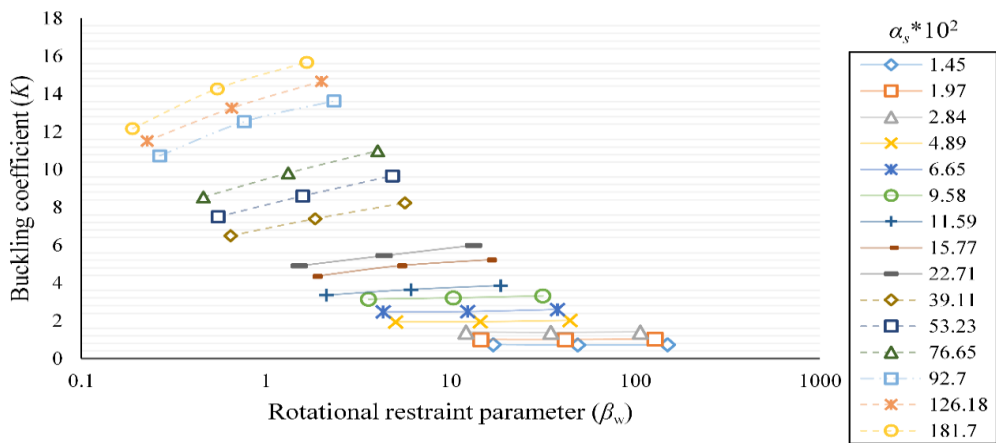
Fig. 9 Variation of buckling coefficient (*K*) with β_w for different α_s values (a) $(D_{11}/D_{22})_w$ = 8.790 (b) $(D_{11}/D_{22})_w$ = 1 (c) $(D_{11}/D_{22})_w$ = 0.114.
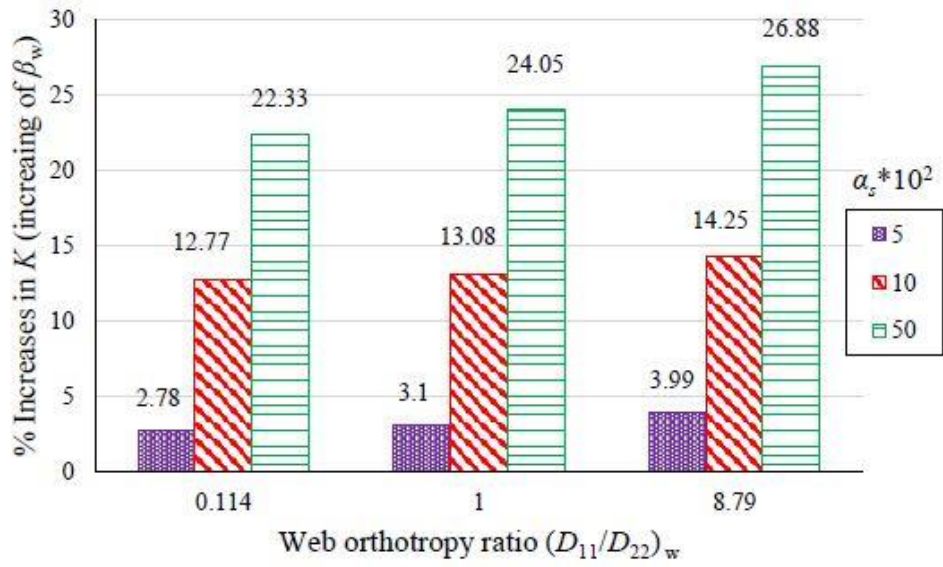
Fig. 10 Influence of β_w on buckling coefficient (K) for different α_s values

(c)

(d)
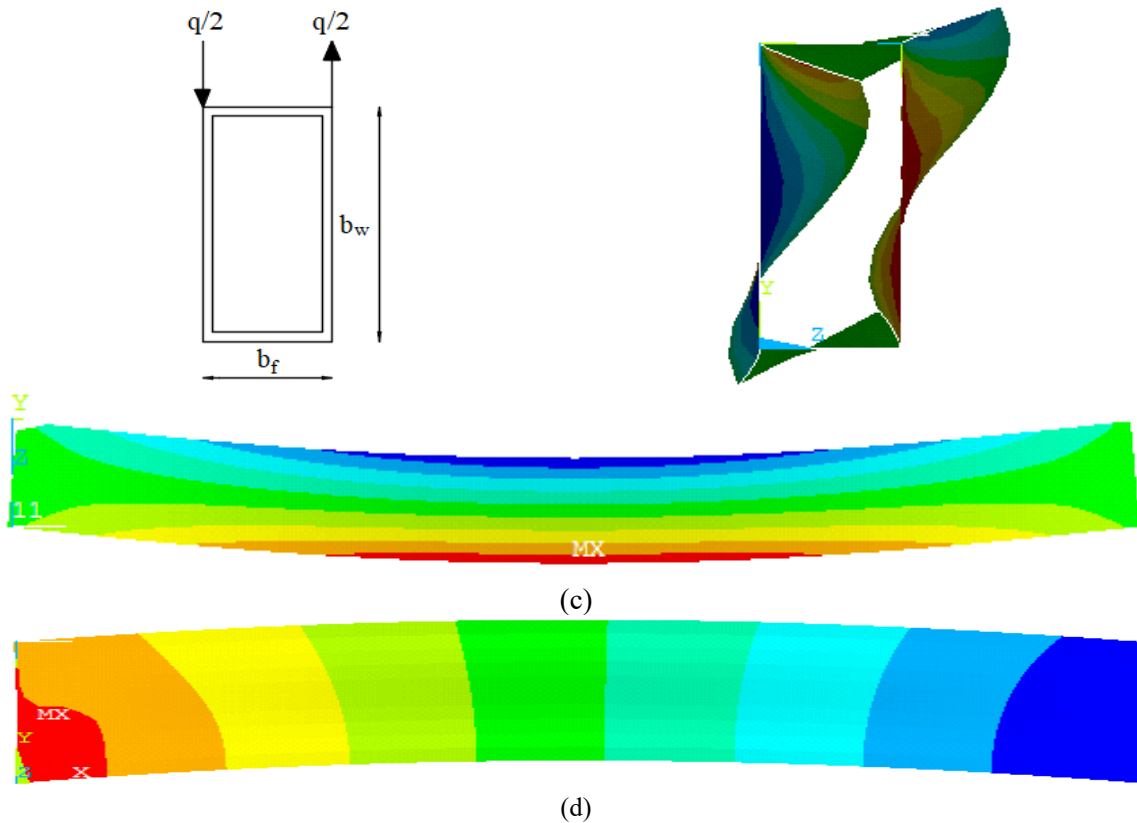
Fig. 11 Box-beam (a) Cross-section with torsional load (b) Deformed shape (c) Stress variation in X-plane (d) Shear stress variation in XY-plane
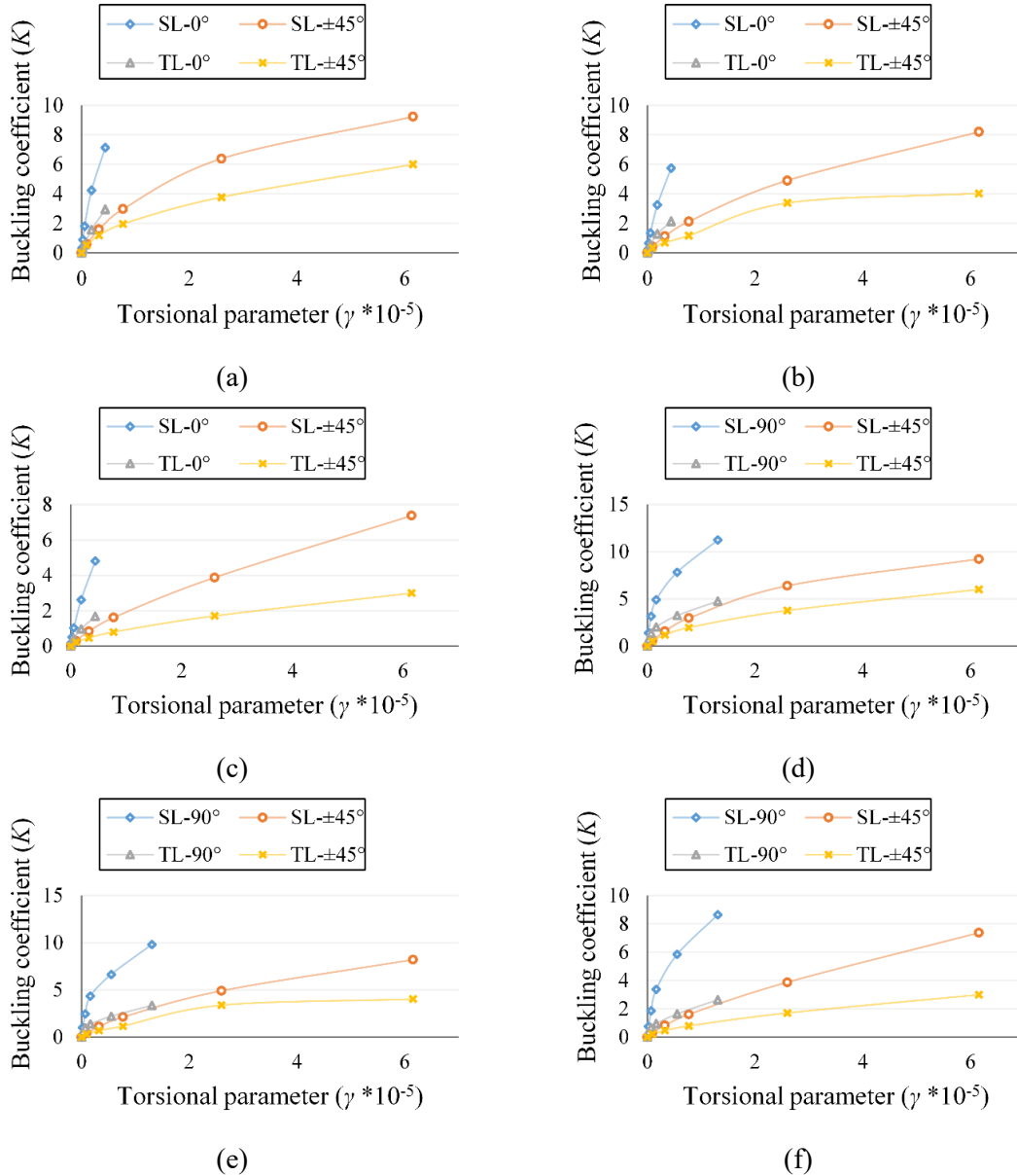
Fig. 12 Buckling coefficient (*K*) versus torsional parameter (*γ*) (a, d) b_w=500 (b, e) b_w=600 (c, f) b_w=700

value of ±45º panel will be much higher than the panels having 0º and 90º fiber orientation in webs.

Fig. 13 shows the significance of the torsional parameter (*γ*) on the buckling coefficient (*K*) under the torsional load case. Whereas, the % increases in buckling coefficient (*K*) when web fiber orientation is changed from 0° and ±45° (increasing of *γ*) is plotted against the corresponding differences in $α_s$ for two types of load cases i.e., *SL* and *TL*. From this figure, it can be observed
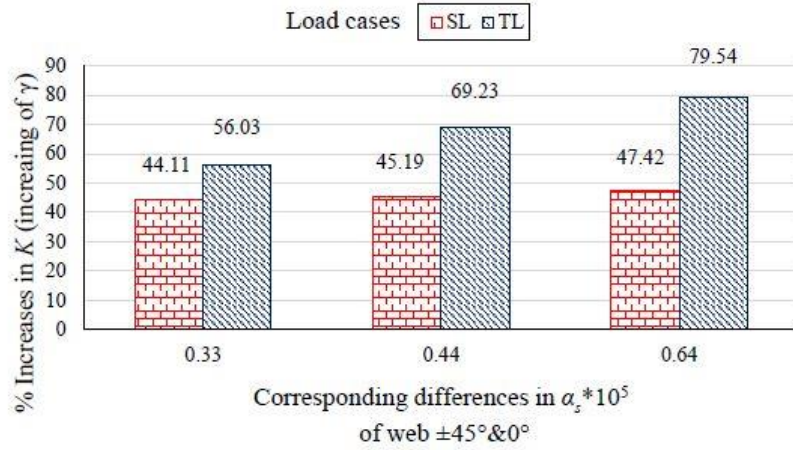
Fig. 13 Effect of γ on buckling coefficient (K) under torsional load

Table 5 Ranges of the geometrical parameters

L (m)	B (m)	b_f (m)	b_w (m)	t_d (mm)	t_w (mm)	t_f (mm)
7.5-15	1.5	0.45	0.6	4-12	8-11.5	4-8

Table 6 Stiffness ratios of the beam components

Components	Stacking sequence (θ, degree)	(D_{11}/D_{22})	(A_{11}/A_{66})
Deck	[90°/±45°/0°]$_s$	0.3006	3.0360
Flange	[90°/0°/0°/0°]$_s$	0.7788	25.481
Web	[90°/±45°/0°/0°]$_s$	0.414	4.5161

that for all the three differences in α_s value, % increases in buckling coefficient (K) under the torsional load case is high for the symmetrical load case. Also, under the torsional load case, γ influence is low at the low difference in α_s value (0.0033). While, at high differences in α_s value (0.0064), γ influence is strong.

6. Demonstration of significance of identified governing parameters and design trends

A simply supported FRP pedestrian bridge with three box-beams as shown in Fig. 14, is considered to show the significance of identified web buckling parameters. Along with the self-weight of the deck, surface load 500 kg/m^2 is applied on the whole area of the bridge deck to simulate the pedestrian loading (IRC: 6-2016). For a constant orthotropy ratio and geometry of different components (flange and web), transverse load capacity for web buckling (at the web-flange junction of box-beam) is calculated by using the proposed design trends. These values are compared with the finite element analysis (FEA) results. The considered geometry ranges and stiffness ratios are shown in Tables 5 and 6. The procedure to obtain transverse loads by using design trends is given below.

(a)

(b)
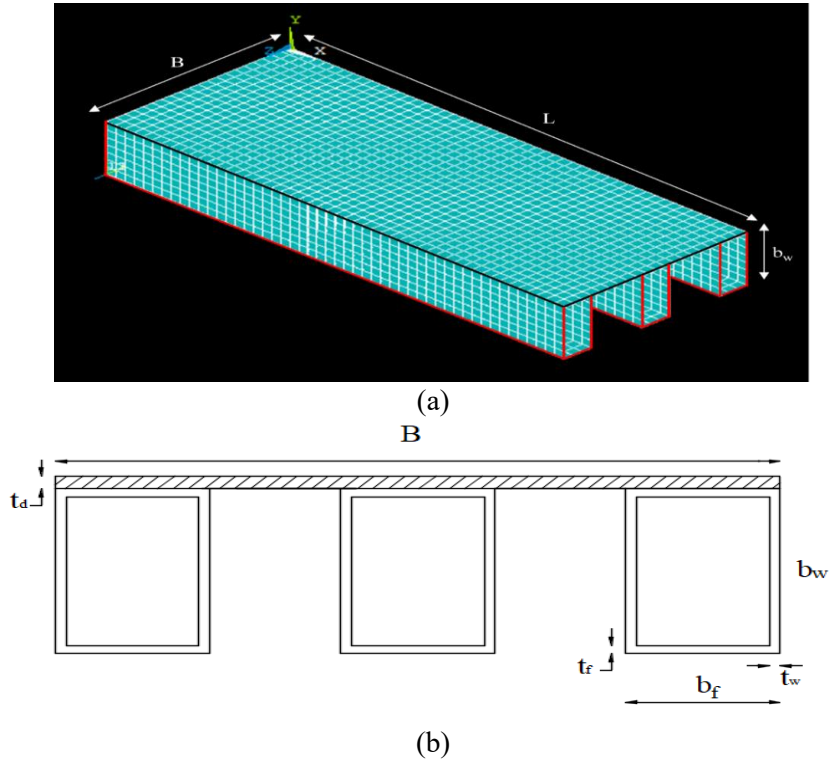
Fig. 14 Schematic view of the FRP deck: (a) Isometric view and (b) Front view

6.1 Transverse load estimation through web buckling parameters

First, for the given geometry and configuration of the box-beams, the values of the web buckling parameters, i.e., α_s and δ_w, are calculated using Eqs. (2) and (4). Then the corresponding buckling coefficient (K) value is obtained from the design trends (refer Fig. 6) for the calculated α_s and δ_w. Further, the in-plane shear force is obtained by using Eq. (6).

$$N_{xy} = K \frac{\pi^2}{b_w} \left(D_{11} D_{22}^3 \right)^{\frac{1}{4}}$$ (6)

Finally, the transverse load (w_u) is obtained by using the following equation

$$w_u = \frac{2N_{xy}}{L}$$ (7)

6.2 Transverse load estimation through finite element analysis

To obtain transverse load at the web-flange junction of the FRP box-beam through finite element analysis (FEA) of the pedestrian bridge, simply supported box-beam, as shown in Fig. 3 is used. The applied line load at web-flange junction corresponds to the pedestrian load of 500 kg/m^2

Table 7 Validation of proposed graph – Transverse load comparison for the pedestrian bridge

Geometry based parameters			Governing parameters		Capacity predictions	
L	$(b/t)_\text{f}$	$(b/t)_\text{w}$	α_s	δ_w	Using governing parameters α_s and δ_w	Using FEA
7.5	125	72.73	9.814	3.836	4.042	4.377
10	105.26	66.15	13.041	3.836	4.078	4.422
12.5	90.91	61.86	15.952	3.836	4.035	4.679
15	80.65	58.25	19.909	3.836	4.073	4.482

is 3.813 kN/m. The applied line load is equally applied over the web-flange junction of box-beam. Then, the transverse load for web buckling is calculated by multiplying the applied load and obtained the buckling factor from the eigen buckling analysis.

6.3 Comparison of results

Table 7 shows the values of the identified parameters and obtained transverse loads. From Table 7, it can be observed that for different L/b_w ratios, the transverse load obtained from the FEA is in good agreement with the predicted transverse loads using proposed trends. This verifies the accuracy of the proposed trends. Further, it indicates that identified parameters and proposed trends can help to design the FRP box-beams.

7. Conclusions

Web buckling is studied earlier also, but most of the works are carried out by using the discrete plate approach. In reality, plates are the part of beams and their buckling strength is significantly influenced by the state of stress and boundary condition at the web-flange junction. Because of this, in this study, web buckling is studied as part of the box beam by modeling full box-beams by using FEA software 'ANSYS 15'. Extensive numerical studies through simulations are conducted by changing the fiber orientation and geometry of flange and web elements. Four parameters influencing the web buckling are identified, i.e., flexural (α_s), rotational restraint (β_w), shear (δ_w) and torsional (γ). The processing of numerical data in the form of curves and bar charts show the influence of various parameters on web buckling. Finally, the significance of governing parameters and design trends is shown by comparing the transverse load of FRP box-beams. Based on this study, the following conclusion giving qualitative and quantitative trends are drawn.

Influence of flexural parameter (α_s) and shear stiffness parameter (δ_w)
• When $\alpha_s < 0.1$, the rate of increase in buckling coefficient with an increase in α_s is high, while the effect of δ_w is insignificant.
• When $\alpha_s > 0.1$, the rate of increase in buckling coefficient with an increase in α_s is low; however, the effect of δ_w becomes significant.
• For the same value of α_s, at higher δ_w, the buckling coefficient will be higher, and in the present study, the maximum increase in buckling coefficient due to δ_w is observed around 16%.
Influence of rotational restraint parameter (β_w)
• Rotational restraint parameter (β_w) is more significant when $\alpha_s > 0.1$. At higher α_s, the

influence of β_w is strong, and in the present study, the maximum increase in buckling coefficient due to β_w is observed around 27%.

Influence of torsional parameter (γ)

• In general, the buckling coefficient increases with an increase in the torsional parameter (γ).

• For the same value of b/t, the maximum value of γ can be achieved by adopting $\pm 45°$ fibers in the web, and the same will be advantageous in case of torsional loading.

Based on the above observations, in general, it can be noticed that α_s is the most significant parameter for web buckling and β_w as well as δ_w enhance buckling performance at a higher value of α_s significantly. The parameters β_w and δ_w depend on properties of the flange as well as the web of the box-beam, and their real effect cannot be simulated by using the discrete plate approach. The parameter γ is found to be significant in the case of torsional loading. Lack of design database is a major issue in the design of laminated composite structures, and the trends coming out of an extensive numerical study done in the present work will be helpful to the designer during the preliminary design of FRP box-beams; it has proved herein by designing the pedestrian bridge.

Funding

References

ANSYS (2003), "User's Manual (Version 15)", *ANSYS, Inc, Canonsburg,* P.A.

Bank, L.C. and Yin, J. (1996), "Buckling of orthotropic plates with free and rotationally restrained unloaded edges", *Thin-Walled Struct.*, **24**, 83-96. https://doi.org/10.1016/0263-8231(95)00036-4.

Barbero, E.J. and Raftoyiannis (1993), "Prediction of buckling-mode Interaction in composite columns", *J. Mater. Civ. Eng*, **5**(3), 339-355. https://doi.org/10.1080/10759410050031130.

Bleich, F. (1952), *Buckling Strength of Metal Structures*, *McGraw-Hill, New York*.

Cardoso, D.C.T., Harries, K.A. and Batista, E.M. (2014), "Closed-form equations for compressive local buckling of pultruded thin-walled sections", *Thin-Walled Struct.*, **79**, 16-22. https://doi.org/10.1016/j.tws.2014.01.013.

Chandak, R. Upadhyay, A. and Bhargava, P. (2008), "Shear lag prediction in symmetrical laminated composite box beams using artificial neural network", *Struct. Eng. Mech.*, **29**(1), 77-89. https://doi.org/10.12989/sem.2008.29.1.077.

Debski, H., Kubiak, T. and Teter, A. (2013), "Buckling and postbuckling behavior of thin-walled composite channel section column", *Compos. Struct.*, **100**, 195-204. https://doi.org/10.1016/j.compstruct.2012.12.033.

Housner, J.M. and Stein, M. (1975), "Numerical analysis and parametric studies of the buckling of composite orthotropic compression and shear panels", *NASA TN D-7996*.

Kasiviswanathan, M. and Upadhyay, A. (2018), "Flange buckling behavior of FRP box-beams: A parametric study", *J. Reinf. Plast. Compos.*, **37**(2), 105-117. https://doi.org/10.1177/0731684417736142.

Kollar, L.P. (2002), "Buckling of unidirectionally loaded composite plates with one free and one rotationally restrained unloaded edge", *J. Struct. Eng.*, **128**, 1202-1211. https://doi.org/10.1061/(ASCE)0733-9445(2002)128:9(1202).

Kollar, L.P. (2003), "Local buckling of fiber reinforced plastic composite structural members with open and closed cross sections", *J. Struct. Eng.*, **129**, 1503-1513. https://doi.org/10.1061/(ASCE)0733-9445(2003)129:11(1503).

Kubiak, T. Kolakowski, Z. Swiniarski, J. Urbaniak, M. and Gliszczynski, A. (2016), "Local buckling and

post-buckling of composite channel-section beams - Numerical and experimental investigations", *Compos. Part B*, **91**, 176-188. https://doi.org/10.1016/j.compositesb.2016.01.053.

Lekhnitskii, S.G. (1968), "Anisotropic plates", *Gorden and Breach Science Publishers,* New York.

Liu, Q., Qiao, P. and Guo, X. (2014), "Buckling analysis of restrained orthotropic plates under combined in-plane shear and axial loads and its application to web local buckling", *Compos. Struct.*, **111**, 540-552. https://doi.org/10.1016/j.compstruct.2014.01.036.

Mallela, K.U. and Upadhyay, A. (2009), "Validity of simplified analysis for the stability of laminated composite stiffened panels subjected to in-plane shear", *Struct. Eng. Mech.*, **32**(4), 583-586. https://doi.org/10.12989/sem.2009.32.4.583.

Qiao, P., Davalos, J.F. and Wang, J. (2001), "Local buckling of composite FRP shapes by discrete plate analysis", *J. Struct. Eng.*, **127**, 245-255. https://doi.org/10.1061/(ASCE)0733-9445(2001)127:3(245).

Qiao, P. and Huo, X. (2011), "Explicit local buckling analysis of rotationally-restrained orthotropic plates under uniform shear", *Compos. Struct.*, **93**(11), 2785-2794. https://doi.org/10.1016/j.compstruct.2011.05.026.

Qiao, P. and Shan, L. (2005), "Explicit local buckling analysis and design of fiber-reinforced plastic composite structural shapes", *Compos. Struct.*, **70**(4), 468-483. https://doi.org/10.1016/j.compstruct.2004.09.005.

Qiao, P. and Zou, G. (2002), "Local buckling of elastically restrained fiber-reinforced plastic plates and its application to box sections", *J. Eng. Mech.*, **128**, 1324-1330. https://doi.org/10.1061/(ASCE)0733-9399(2002)128:12(1324).

Qiao, P. and Zou, G. (2003), "Local buckling of composite fiber-reinforced plastic wide-flange sections", *J. Struct. Eng.*, **129**(1)**,** 125-129. https://doi.org/10.1061/(ASCE)0733-9445(2003)129:1(125).

Ranganathan, S. and Mantena, R. (2003), "Axial loading and buckling response characteristics of pultruded hybrid glass-graphite/epoxy composite beams", *J. Reinf. Plast. Compos.*, **22**, 671-689. https://doi.org/10.1177/073168403024566.

Sathiyaseelan, S. and Baskar, K. (2012), "Numerical study on thin plates under the combined action of shear and tensile stresses", *Struct Eng. Mech.*, **42**(6), 867-882. https://doi.org/10.12989/sem.2012.42.6.867.

Serror, M.H., Hamed, A.N. and Mourad, S.A. (2016), "Numerical study on buckling of steel web plates with openings", S*teel. Compos. Struct.*, **22**(6), 1417-1443. https://doi.org/10.12989/scs.2016.22.6.1417.

Stroud, W.J. and Agranoff, N. (1976), "Minimum-mass design of filamentary composite panels under combined loads: Design procedure based on simplified buckling equations", *NASA TN D-8257*.

Taleb, C.E., Ammari, F. and Adman, R. (2015), "Analytical study of buckling profile web stability", *Struct. Eng. Mech.*, **53**(1), 147-158. https://doi.org/10.12989/sem.2014.53.1.147.

Tarjan, G., Sapkas, A. and Kollar, L.P. (2010a), "Stability analysis of long composite plates with restrained edges subjected to shear and linearly varying loads", *J. Reinf. Plast. Compos.*, **29**(9), 1386-1398. https://doi.org/10.1177/0731684409105078.

Tarjan, G., Sapkas, A. and Kollar, L.P. (2010b), "Local web buckling of composite (FRP) Beams", *J. Reinf. Plast. Compos.*, **29**(10), 1451-1462. https://doi.org/10.1177/0731684409105083.

Upadhyay, A. and Kalyanaraman, V. (2003), "Simplified analysis of FRP box-girders", *Compos. Struct.*, **59**, 217-225. https://doi.org/10.1016/S0263-8223(02)00195-2.

Whitney, J.M. (1987), "Structural analysis of laminated anisotropic plates", *Technomic, Lancester.*

Zhan, Y. Wu, G. and Harries, K. A. (2018), "Determination of critical load for global flexural buckling in concentrically loaded pultruded FRP structural struts", *Eng. Struct.*, **158**, 1-12. https://doi.org/10.1016/j.engstruct.2017.12.008.

Zhan, Y. and Wu, G. (2018), "Determination of critical loads for global buckling of axially loaded pultruded fiber-reinforced polymer members with doubly symmetric cross sections", *Adv. Struct. Eng.*, **21**(12), 1-12. https://doi.org/10.1177/1369433218759572.

WT

Notations

L	beam length
t_w, t_f	thickness of web and flange
b_w, b_f	width of web and flange
k_s	shear loaded panel buckling factor
K	buckling coefficient
SL	symmetric load
TL	torsional load
δ_w	shear stiffness parameter
β_w	rotational restraint parameter
γ	torsional parameter
α_s	flexural parameter for shear loaded panel
E_1, E_2, G_{12}	lamina modulus
υ_{12}, υ_{21}	lamina major and minor Poisson's ratio
θ_f, θ_w	fiber orientation of flange and web
D_{11}, D_{22}, D_{12}, D_{66}	orthotropic bending stiffness